ACTUARIAL RESEARCH CLEARING HOUSE
1994 VOL. 1

CHAOTIC ANALYSIS ON U. S. TREASURY INTEREST RATES

BY

STEVE CRAIGHEAD

ABSTRACT: This paper analyzes the U. S. Treasury monthly interest rates from 1953 to 1992, and the daily rates from 1981 to 1992 for various forms of chaotic behavior. The primary analysis was in determining the Hurst Exponent by the use of Rescaled Range Analysis. The Hurst Exponent will be used to consider the efficiency of the Treasury Market. This paper also discusses other possible uses of Fractional Brownian Motion in Finance Theory, Macroeconomics, and Actuarial Science.

Keywords: Brownian Motion, Fractional Brownian Motion, Interest Rates, Efficient Market Hypothesis, Rescaled Range Analysis, Hurst Exponent

Predicting interest rates or the direction of their movement has been and continues to be an ongoing problem in the financial world. This paper takes a hard look at that problem from the perspective of Chaos. This presentation does not include extensive detail on the fundamentals of Fractals in Chaos Theory, which is quite adequately done in [1],[2], and [3].

The outline of this paper is as follows:

Section 1. Description of Data.

Section 2. Discussion of Deterministic Chaos and analysis of ninety day daily interest time series. Also contained is a discussion of possible hidden cycles in this data.

Section 3. Discussion of Fractional Brownian Motion and the Hurst Exponent.

Section 4. Rescaled Range Analysis

Section 5. Empirical Results.

Section 6. Conclusions and Further Research.

Section 1. Description of Data.

We empirically examine the fcllowing four time series in this paper:

A. The 90 Day T-Bill Daily rates from May 1, 1981 through April 30, 1992 (a total of 2,704 data points). These rates are at bond equivalent value, allowing a proper comparison with the ten year rates. See [4].

B. The 90 Day T-Bill Monthly rates from April 30, 1953 through December 31, 1992. These rates are also at bond equivalent value.

C. The 10 Year T-Note Daily rates from May 1, 1981 through April 30, 1992.

D. The 10 Year T-Note Monthly rates from April 30, 1953 through December 31, 1992.

The source of these rates are [5], [6], and [7].

The graphs of the time series A, B, C, and D, along with their first differences, denoted δA, δB, δC, and δD are displayed in Figures 1 and 2.

Section 2. Deterministic Chaos

In deterministic chaos, normally one takes a time series X(t) and embeds the series into a low dimensional vector space of dimension m by examining vectors of the form

$$(X(t), X(t+\tau), X(t+2\tau), \ldots, X(t+(m-1)\tau).$$

where τ is some increment in time. Let this vector be denoted x(t). Next, one can examine the behavior of the path or orbit that these vectors take in the vector space as t changes. If the dynamic system that generates X(t) converges, the orbit will spiral to a point. If the dynamic system is periodic, the orbit will form a closed path. If the dynamic system diverges to infinity, the orbit will spiral out to infinity. Now, some dynamic systems will not converge nor diverge, yet appear to generate random numbers. The orbit traced out is called a

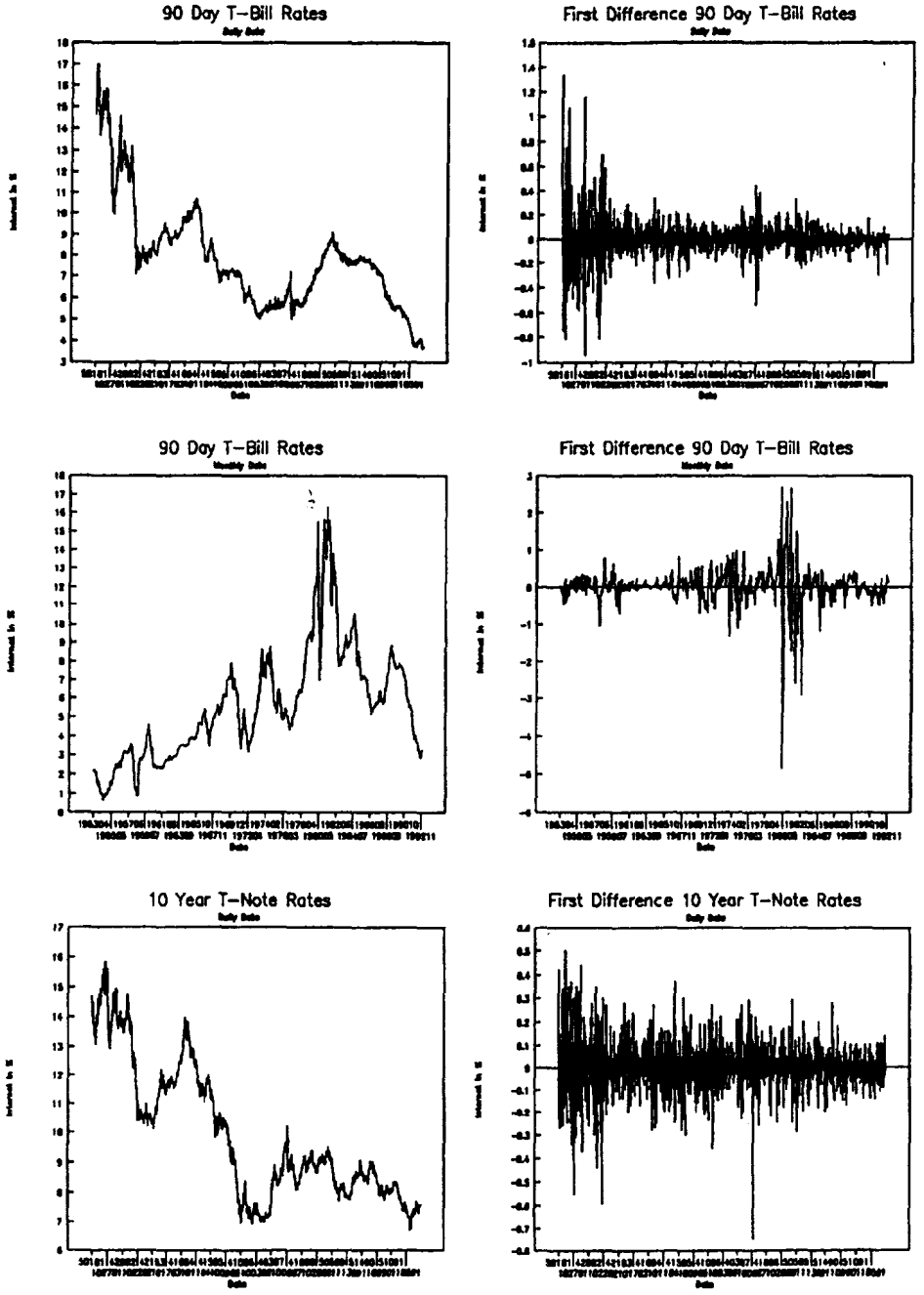
90 Day T-Bill Rates
First Difference 90 Day T-Bill Rates
90 Day T-Bill Rates
First Difference 90 Day T-Bill Rates
10 Year T-Note Rates
First Difference 10 Year T-Note Rates

Figure 1

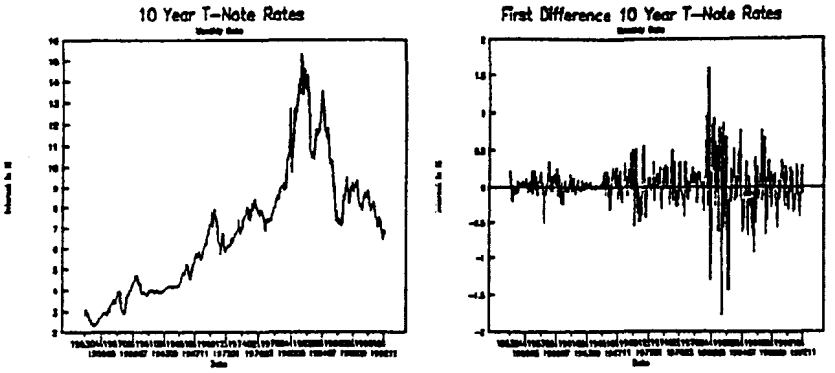

Figure 2

strange attractor. Here the orbit follows a "strange" trajectory that never crosses back over itself. However, this trajectory could be contained in a low dimensional vector space. Though the trajectory may never repeat a path, different times on the trajectory may be very close to other points and they track near one another for a period. If this is the case, one could predict several values into the future, based on the performance of these neighbors. See references [8] through [20], for more details.

There are several algorithms that allow time series analysis to see if the data follows a low dimensional strange attractor. Examples include the determination of the Lyapunov Spectrum, the Correlation Dimension, or other various predictor models. The Lyapunov Spectrum, if determined, summarizes or classifies the strange attractor. The information dimension is derived from the Lyapunov Spectrum. The information dimension gives a rate of loss of information. This rate of loss is used to determine how

far into the future one can predict from a strange attractor's orbit, before information loss dominates the prediction process. In trying to determine the Lyapuncv Spectrum, for δA, the algorithms would not converge, for $m < 10$. The calculation time for higher m was prohibitive and hence was not considered. See [8], [9], [10], [11], [14], and [15] for further discussions. To determine the Correlation Dimension mentioned in [15], and [21], let N(r) be the number of pairs of vectors (x(i),x(j)) whose Euclidian distance is less than r. The Correlation Dimension will then be

$$\lim_{r \to 0} \frac{\ln(N(r))}{\ln(r)}$$

If this converges, the data has a scale invariance. Time scale invariance is discussed futher in Section 3. The predictor models provide measures of ability to predict from the orbit. See [12], [13], [16], and [17]. With these models, when looking for low dimensional orbits, one usually creates some statistic, such as the Correlation Dimension on the trajectory and examines that statistic as one increases the dimension m. If the orbit can be contained in a low dimensional vector space, the statistic will start at some level, for $m = 1$, and rise or fall as m increases. At some point, as the dimension m increases, the statistic will reach a plateau. After reaching this plateau, an increase in m produces little effect.

Studying δA, none of the various deterministic chaotic algorithms, referenced above, reach a plateau. Interestingly,

the highest Correlation Dimension obtained is 0.06 for m=6. However, as m increases past 6, the Correlation Dimension drops and never regains that level. When we examine δA, by other methods later, we will compare to this number. The practical result of the failure of these statistics is that there is little hope to obtain a deterministic model that can predict interest rate changes within δA.

Analyzing the power spectrum of the time series δA for cyclic behavior, there appeared several high frequency cycles. However, autocorrelation analysis suggested no revelevant cycles at these frequencies. Mandelbrot and Wallis mentioned this problem in [22]. Also, an overdetermined autoregressive model, constructed from all 2703 autocorrelation coefficents for δA, produced poor predictions for the prediction period chosen (May 1992). The model predicted that rates would rise when they actually dropped and vice versa. The maximum error was 12 bp; the minimum error was -23bp. Again, for comparison, the autocorrelations for δA, ranged from -.07 to .12.

Attempting to predict interest rates by using a Neural Network model, the predictive ability of the model degraded as the learning time increased, when processing the daily time series from 1981 through 1992. This model consisted of the current ninety-day rate as the output, and the entire previous three days yield curves for input.

At this point any confidence in obtaining a cyclic or deterministic model for the prediction of δA turns to the possibility of noise. This could be also reasoned from the Efficent Market Hypothesis. If a method existed that predicted interest rate changes, the forecast would create an arbitrage opportunity and the predicted value would immediately be reflected in the current rate. This correspondes to Maurice Kendall's results in trying to predict how the stock market moved in his 1953 research. See [36] for a brief summary of his results and a discussion of the Efficient Market Hypothesis.

The method used to analyze the data for noise is called Rescaled Range Analysis (R/S Analysis). Rippi originally developed this technique for reservoir design, and Harold Edwin Hurst improved it for his analysis of the Nile River and its water storage problems. Mandelbrot and Van Ness in [23] and Mandlebrot and Wallis in [22], [24], [25], [26], and [27], generalized these methods in developing Fractional Brownian Motion. We will use Rescaled Range Analysis and the Hurst Expontent as a possible measure of the efficiency of the Treasury Bill and Note Market.

Section 3. Fractional Brownian Motion

In 1827, Scottish botanist Robert Brown described the motion of pollen under a microscrope as a physical and not a biological phenomenon. Now, we refer to this activity as Brownian motion.

Beginning in 1905, Albert Einstein and others used Brownian motion to model diffusion at an atomic level. Later in 1923, Norbert Wiener completely characterized the process, which we now term a Wiener Process. Briefly, one dimensional Brownian motion exists when the incremental change in position of some particle at time t from time t_0 is directly proportional to a normal Gaussian random sample * times the absolute value of the difference in time $|t-t_0|$ to the H'th power where H = ½. That is:

$$B_H(t) - B_H(t_0) \alpha * | t - t_0 |^H \qquad (3.1)$$

Brownian motion exhibits several properties of interest here. One such property is that the motion has average increments of zero. This implies that Brownian motion through time will on average return to the starting position of the time series. This is similar to the concept of mean reversion.

Second, the variance of the increments will diverges with time. See [28] for a more extensive presention of these two properties.

Third, Brownian motion is time scale invariant. Mandelbrot described this property in [29]:

> "To define a scaling noise in intuitive fashion, let us recall that any natural fluctuation can be processes to be heard--as implied by the term noise. Tape it, and listen to it through a speaker that reproduces faithfully between, say, 40 Hz to 14,000 Hz. Then play the same tape faster or slower

> than normal. In general, one expects the character of what is heard to change considerably. A violin, for example, no longer sounds like a violin. And a whale's song, if played fast enough, changes from inaudible to audible. There is a special class of sounds, however, that behave quite differently. After the tape speed is changed, it suffices to adjust the volume to make the speaker output 'sound the same' as before. I propose that such sounds or noises be called scaling."

The last property that we will discuss, is that Brownian motion involves no memory effect. One incremental change is independent of another.

Mandelbrot, Van Ness, and Wallis generalized Brownian motion in formula (3.1), to Fractional Brownian motion, denoted FBM, where H could take on values between 0 and 1 inclusive. Mandelbrot called H the Hurst Exponent in honor of Harold Hurst's work.

FBM also has three of the above properties, namely average zero increments, diverging variance, and time scale independence. However, FBM has a memory effect which depends on the value of H. When $H = \frac{1}{2}$, you just have Brownian motion. When $\frac{1}{2} < H \leq 1$, FBM will be persistent. That is, if the trend has been positive in the immediate past there is a high probability that it will continue to rise. If the trend is negative, it will tend to continue to fall. When $0 \leq H < \frac{1}{2}$, FBM will be anti-persistent. That is, if the trend has been positive in the immediate past there is a high probability that it will become negative. Conversely, if negative, it will tend to reverse to a positive direction. Mandelbrot coined the this persistent behavior as the

Noah and Joseph effects. See [30] for his discussion of the Joseph and Noah effect, as they relate to this long term memory effect.

The long-term memory can be measured by the long-term correlation which is $2^{(2H-1)} - 1$. So if H=.5, the correlation is 0. This type of correlation is not related in the sense of autocorrelation, when one term is related to another term, but this correlation is long-term, spanning many periods. See [31].

Feder generated in [32], three examples of FBM with Hurst exponents H at 0.5, 0.7 and 0.9, by using the following approach:

> "Let $B_H(t)$ represent a FBM dependent upon Hurst Exponent H. Let M represent the memory of the process. Let $t=n\tau$, where τ represents the smallest time interval of the process. Let $\{\phi_i\}$ with $i = 1,2,\ldots,M,\ldots$, be a set of Gaussian random variables with unit variance and zero mean. Let the discrete fractional Brownian increments be generated as follows:
>
> $$B_H(t) - B_H(t-1) = \frac{n^{-H}}{\Gamma(H+\frac{1}{2})}\left[\sum_{i=1}^{nt} (i)^{H-\frac{1}{2}}\phi_{(1+n(M+t)-i)} + \sum_{i=1}^{n(M-1)} ((n+i)^{H-\frac{1}{2}} - (i)^{H-\frac{1}{2}})\phi_{(1+n(M-1+t)-i)}\right] \quad (3.2)$$
>
> Let $B_H(0)$ be equal to the most current value of the time series that is being modelled. By using the above generation of the increments, you can cumulate the values and generate the Fractional Brownian series $B_H(t)$."

Feder's figures 9.4 and 9.5 are duplicated in Figure 3.

Feder mentions that formula (3.2) works best for values of H near 0.5. Feder also states that Mandelbrot's method in [33] is faster than (3.2).

To calculate an H value for a specific time series, one must conduct Rescaled Range Analysis on the series. This analysis is designed to examine the behavior of the time scale invariance.

Section 4. Rescaled Range Analysis

Let X(t) be a stationary time series with T values. Assume that the time series is uniformly spaced in time from t = 1 to t = T. Define the cumulated time series $X^*(t)$ as follows:

$$X^*(t) = \sum_{u=1}^{t} X(u) \qquad (4.1)$$

$X^*(t)$ correspond to $B_H(t)$ in Section 3. Now $s^{-1}X^*(s)$ is the average of the first s values and $s^{-1}[X^*(t+s)-X^*(t)]$ is the average of the values of X(t) between time t+1 and t+s.

$$\text{Define} \quad S^2(t,s) = s^{-1} \sum_{u=t+1}^{t+s} X^2(t) - \left[s^{-1} \sum_{u=t+1}^{t+s} X(u) \right]^2 \qquad (4.2)$$

$S^2(t,s)$ becomes the sample variance of the values of X(t) between time t+1 and t+s.

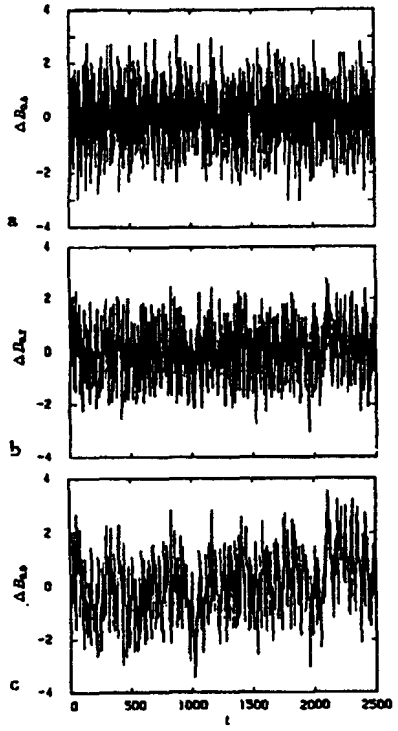

FIGURE 9.4: Fractal noise or increments of the fractal Brownian function B_H evaluated with $M = 700$, $n = 8$. (a) Ordinary Brownian increments for $H = 1/2$. (b) Fractional increments for $H = 0.7$. (c) Fractional increments for $H = 0.9$.

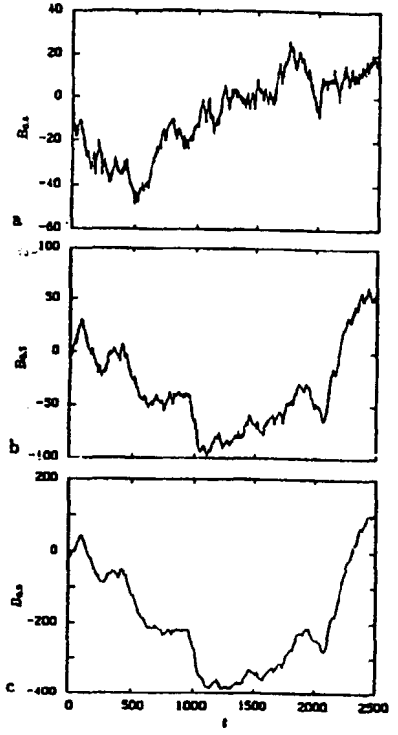

FIGURE 9.5: The fractal Brownian function B_H evaluated with $M = 700$, $n = 8$ and with $B_H(0) = 0$. (a) The ordinary Brownian function for $H = 1/2$. (b) Fractional Brownian function for $H = 0.7$. (c) Fractional Brownian function for $H = 0.9$.

Figure 3.

Let $X^{t,s,u}$ be defined as:

$$X^{t,s,u} = X^*(t+u) - X^*(t) - \frac{u}{s}[X^*(t+s) - X^*(t)] \quad (4.3)$$

for $0 \le u \le s$.

$X^{t,s,u}$ is the cumulated departure at time t+u from the average between time t+1 and t+s.

Define R(t,s) as follows:

$$R(t,s) = \max_{0 \le u \le s} \{ X^*(t+u) - X^*(t) - \frac{u}{s}[X^*(t+s) - X^*(t)] \} - \min_{0 \le u \le s} \{ X^*(t+u) - X^*(t) - \frac{u}{s}[X^*(t+s) - X^*(t)] \} \quad (4.4)$$

or equivalently

$$R(t,s) = \max_{0 \le u \le s} \{ X^{t,s,u} \} - \min_{0 \le u \le s} \{ X^{t,s,u} \} \quad (4.5)$$

R(t,s) is the range of the cumulated departure between time t+1 and t+s.

Define the R/S statistic as

$$R/S(t,s) = R(t,s)/S(t,s) \quad (4.6)$$

Mandlebrot and Wallis in [27], showed the following method of determining H with Rescaled Range analysis was robust:

Create a collection of $R(t,s)/S(t,s)$ for a various s over different times $t_{s,i}$, where $(t_{s,i})$ will vary based on s. Then find the expectation of these $R(t_{s,i},s)/S(t_{s,i},s)$ for each s. Let this expectation be denoted $E[R/S(s)]$. If

$$\lim_{s\to\infty} s^{-H} E[R/S(s)] \text{ is finite and positive}$$

then the time series satisfies the s^H law in the mean. Next, estimate H to be $\ln(E[R/S(s)])/\text{Log}(s)$, by doing a linear regression between $\ln(s)$ and $\ln(E[R/S(s)])$, assuming a zero intercept. Mandlebrot and Walis and Feder in [27] and [34] go into further detail on the analysis of the results of the regression. This type of analysis is of data differs substantially from that of standard ARIMA analysis. In ARIMA analysis the statistician is attempting to split the behavior of the time series into a cyclical component and into a noise component. The chaotic approach using in this paper, however treats the data holistically in that it does not try to create this distinction.

Mandlebrot and Wallis in [22] and [26], and Feder in [35] discusses that values of $\ln(E[R/S(s)])$ have certain properties based on the location of $\ln(s)$. When $s < 20$, the values for $\ln(E[R/S(s)])$ are considered random and should not be taken into consideration, when doing the regression analysis. Mandlebrot argues that this is because that for $s < 20$, the various statistics generated for the derivation of $\ln(E[R/S(s)])$, have Student t distributions, and the s^H Law of the Mean begins to

show its influence at s=20 due to the Law of Large Numbers. The second region is the actual region that reveals the long term correlation or memory effect. Mandlebrot hypothesized that this was for values of s between 20 and 10,000. However, Feder in [35] observed that the memory effect ended when s was near 4,000. For s above this upper bound, the FBM, returns to pure Brownian motion with H=½.

Section 5. Empirical Results

To convert the time series, A, B, C, and D into stationary time series, we first obtain the sample means and variances for each of the time series. Next, we derive the time series A', B', C', and D', by subtracting the sample means from each value in the respective time series and dividing those results by the respective sample standard deviations. Taking first differences produces the time series δA', δB', δC', and δD'.

Mandlebrot and Wallis in [22], discusses the choice of the various s and t to calculate E[R/S(s)]. Roughly following their approach, the list of s for daily time series analysis was {3, 4, 5, 10, 15, 20, 25, 30, 45, 50, 60 75, 100, 200, 220, 300, 600, 900, 1000, 1800, 2700}. For the s values from 3 through 100 the list of t was {1, 100, 200, 300, ..., 2600}. For s = 200, t was {1, 100, 200, ..., 2500}. For s = 220 and 300, t took on values {1, 100, 200, ..., 2400}. For higher s < 2700, t was {1, 100,

200, ..., 2700 -s). For s = 2700, t was singularly (1). The list of s for the monthly time series analysis was (3, 4, 5, 10, 15, 20, 25, 30, 45, 50, 60, 75, 100, 200, 220, 300, 450). For s from 3 to 25, t was (1, 25, 50, ..., 450). For s = 30 to 50, t was (1, 25, 50, ..., 425). For s = 60 and 75, t was (1, 25, 50, ..., 400). For s = 100, 200, and 300, t was (1, 25, 50, ..., 475-s). For s = 220, t was (1, 25, 50, ..., 250). Finally, for s = 474, t was taken as 1. The only deviation from their method was the choice of t = 220. This value was chosen because earlier spectral analysis of the time series pointed to a possible hidden cycle of 220. This was later discredited, as noted in section 2. However, the value for t was not removed from the R/S analysis, and should not have any effect.

Tables 1 through 4 show ln(s) and ln(E[R/S(s)] that are generated from the above values of s and t.

Table 1
Daily 90 Day Rates $\delta A'$

s	ln(s)	ln(E[R/S(s)]
3	1.09861	.30469
4	1.38629	.50134
5	1.60944	.67257
10	2.30259	1.15113
15	2.70805	1.38467
20	2.99573	1.60471
25	3.21888	1.73996
30	3.40120	1.79715
45	3.80666	2.02860
50	3.91202	2.07937
60	4.09434	2.22787
75	4.31749	2.35396
100	4.60517	2.50148
200	5.29832	2.87622
220	5.39363	2.97845
300	5.70378	3.15794
600	6.39693	3.55955
900	6.80239	3.89229
1000	6.90776	3.97081
1800	7.49554	4.20186
2700	7.90101	4.35134

Table 2
Monthly 90 Day Rates $\delta B'$

s	ln(s)	ln(E[R/S(s)]
3	1.09861	.30983
4	1.38629	.55008
5	1.60944	.72638
10	2.30259	1.22795
15	2.70805	1.49911
20	2.99573	1.71054
25	3.21888	1.80269
30	3.40120	1.97925
45	3.80666	2.30833
50	3.91202	2.35081
60	4.09434	2.47558
75	4.31749	2.55761
100	4.60517	2.60225
200	5.29832	2.80264
220	5.39363	2.86771
300	5.70378	2.92191
474	6.16121	3.33171

Table 3
Daily 10 Year Day Rates δC'

s	ln(s)	ln(E[R/S(s)]
3	1.09861	.29437
4	1.38629	.49005
5	1.60944	.66372
10	2.30259	1.14330
15	2.70805	1.43130
20	2.99573	1.55976
25	3.21888	1.66568
30	3.40120	1.77145
45	3.80666	2.03999
50	3.91202	2.06084
60	4.09434	2.19469
75	4.31749	2.33521
100	4.60517	2.50189
200	5.29832	2.98394
220	5.39363	3.04531
300	5.70378	3.17404
600	6.39693	3.59927
900	6.80239	3.87431
1000	6.90776	3.94280
1800	7.49554	4.21440
2700	7.90101	4.17657

Table 4
Monthly 10 Year Rates D'

s	ln(s)	ln(E[R/S(s)]
3	1.09861	.30245
4	1.38629	.51656
5	1.60944	.62239
10	2.30259	1.21344
15	2.70805	1.43115
20	2.99573	1.63733
25	3.21888	1.76492
30	3.40120	1.91515
45	3.80666	2.17146
50	3.91202	2.22468
60	4.09434	2.35153
75	4.31749	2.43283
100	4.60517	2.59845
200	5.29832	2.29265
220	5.39363	2.94253
300	5.70378	3.15356
474	6.16121	3.56516

Figures 4 through 7 illustrate pox diagrams for the A' time series. (Mandlebrot and Wallis introduces pox diagrams in [22].) Figure 4 shows the log-log Ln(s) vs Ln(R/S(s,t)), with a line drawn through Ln(E[R/S(s)]) for each s. In Figure 5, includes the line H=.5. Note that the bulk of the pox are above the H=.5 line. Figure 6 overlays the regressed line of H=.553. This addition completes the pox diagram. Finally, Figure 7 shows the diagram with the pox. Figures 8 through 13 show corresponding diagrams for the other time series.

Note the lighting bolt shape of the Ln(s) vs Ln(E[R/S(s)) graph in either figure 8, or 9. There are three possible reasons for this behavior. Mandlebrot and Wallis in [27], discusses the potential of cycles contained within the data. However, ARIMA analysis (see section 2) precluded the cycle possiblity. The second possibility is that the data is moving into the third region where the memory effect weakens. However, the memory effect is not declining, since the graph moves back to the H=.556 line for high s values. The third possiblity is the higher volatility in the monthly ninety-day rates. Higher volatility could very well cause the high standard error of the Y estimate, and the lower R^2 value. The graphs corresponding to the other three time series δB, δC, and δD, have smaller standard errors and higher R^2, and their Ln(s) vs Ln(E[R/S(s)) graphs, do not meander about the regressed H line as δA'.

The following chart is a summary of the the data

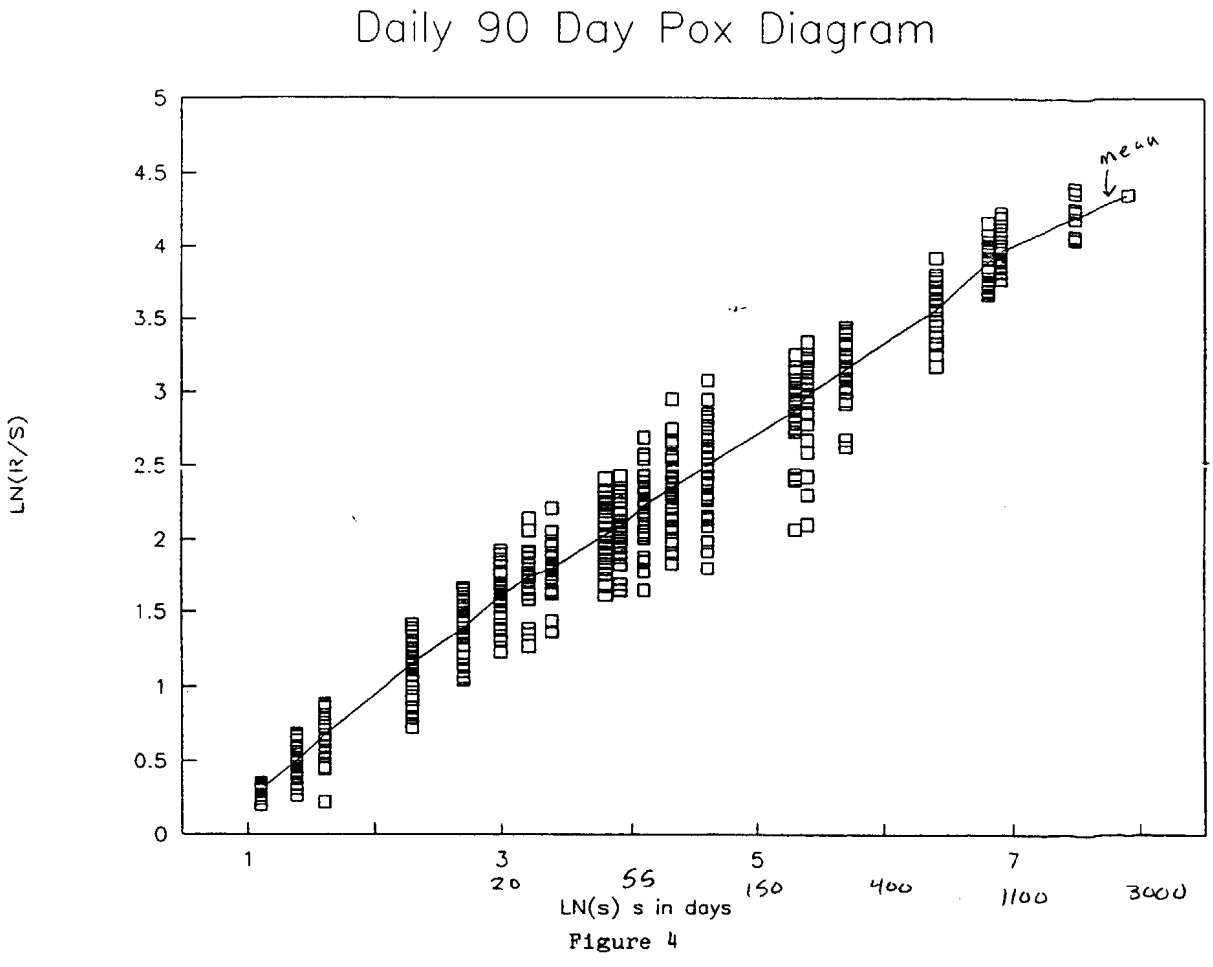
Daily 90 Day Pox Diagram
LN(R/S)
5
4.5
4
3.5
3
2.5
2
1.5
1
0.5
0
mean
1
3
20
55
5
150
400
7
1100
3000
LN(s) s in days

Figure 4

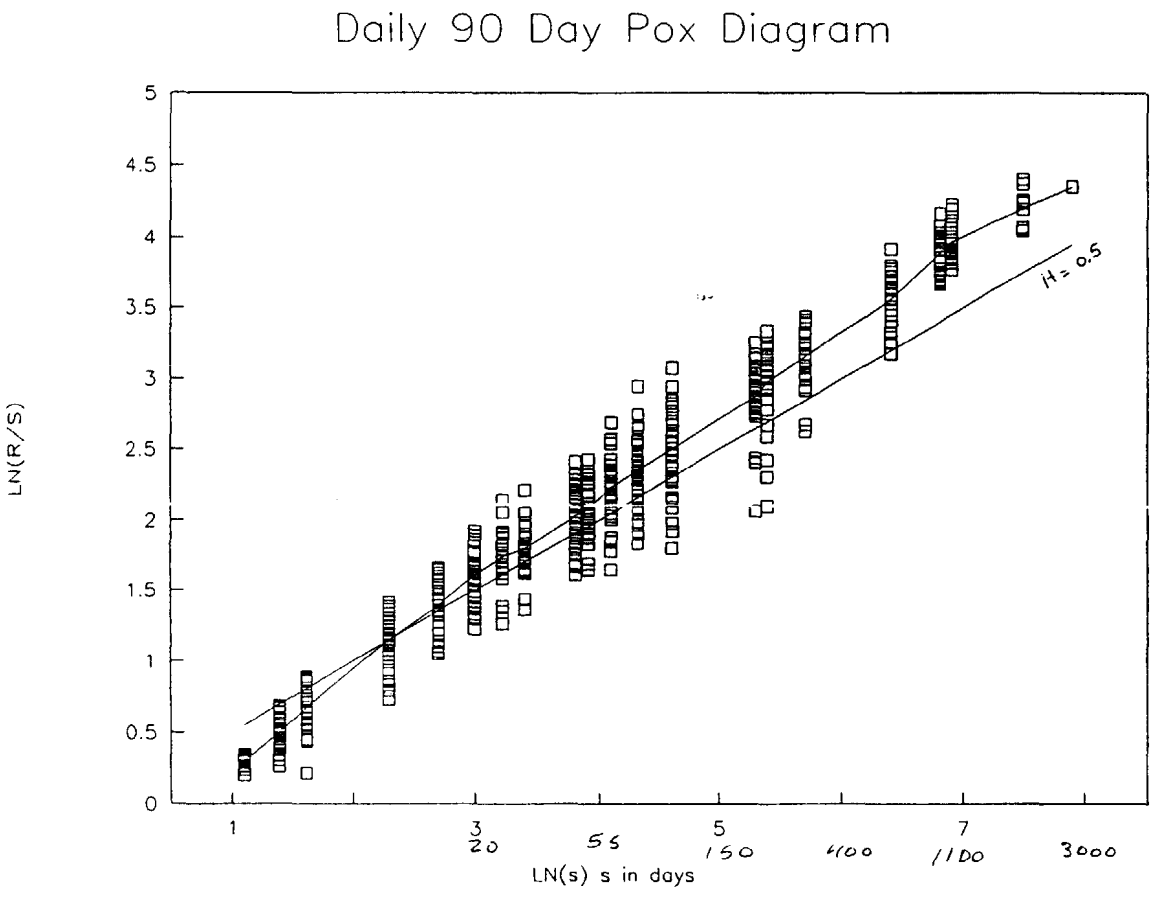
Daily 90 Day Pox Diagram
LN(R/S)
5
4.5
4
3.5
3
2.5
2
1.5
1
0.5
0
H = 0.5
1
3
20
55
5
150
400
7
1100
3000
LN(s) s in days

Figure 5

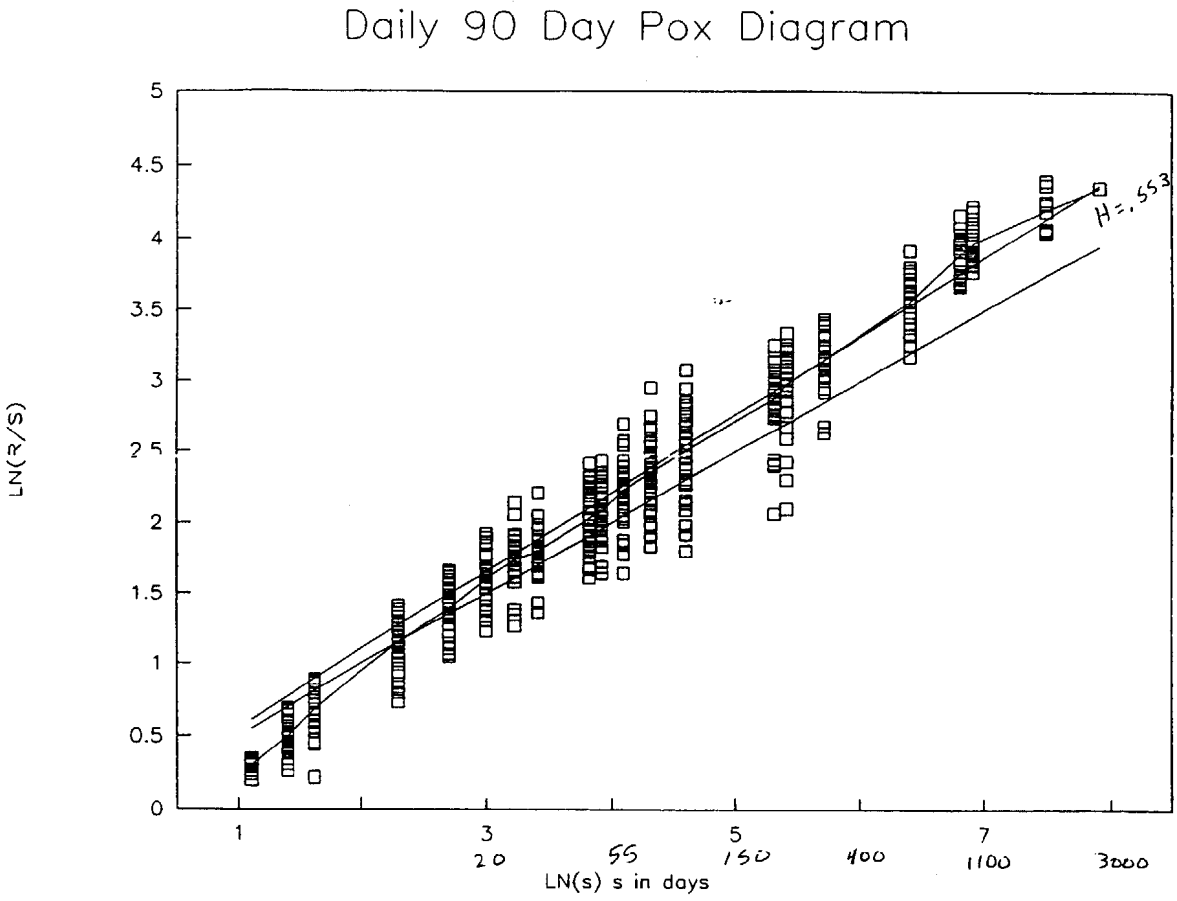
Daily 90 Day Pox Diagram
LN(R/S)
5
4.5
4
3.5
3
2.5
2
1.5
1
0.5
0
H=.553
1
3
20
55
5
150
400
7
1100
3000
LN(s) s in days

Figure 6

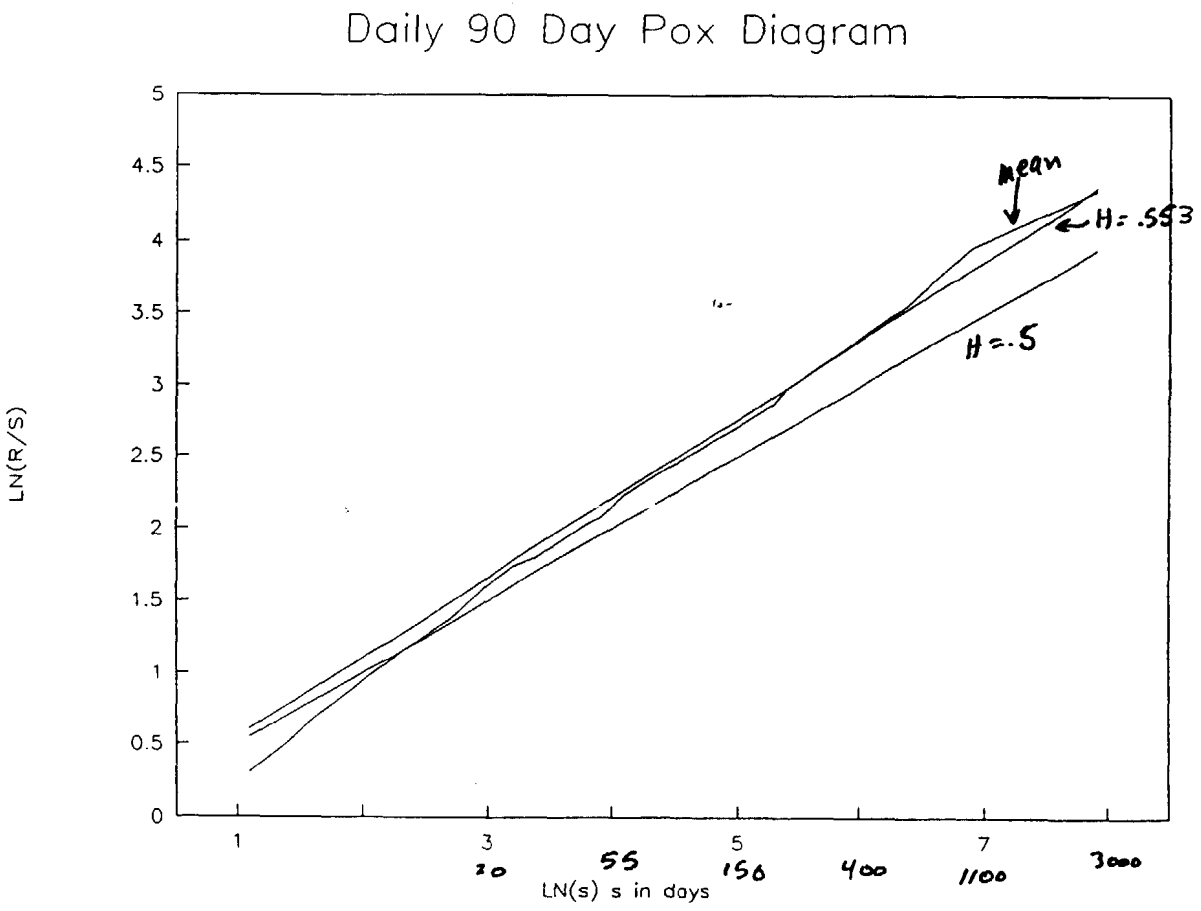
Daily 90 Day Pox Diagram
LN(R/S)
5
4.5
4
3.5
3
2.5
2
1.5
1
0.5
0
Mean
H=.553
H=.5
1
3
5
7
20
55
150
400
1100
3000
LN(s) s in days

Figure 7

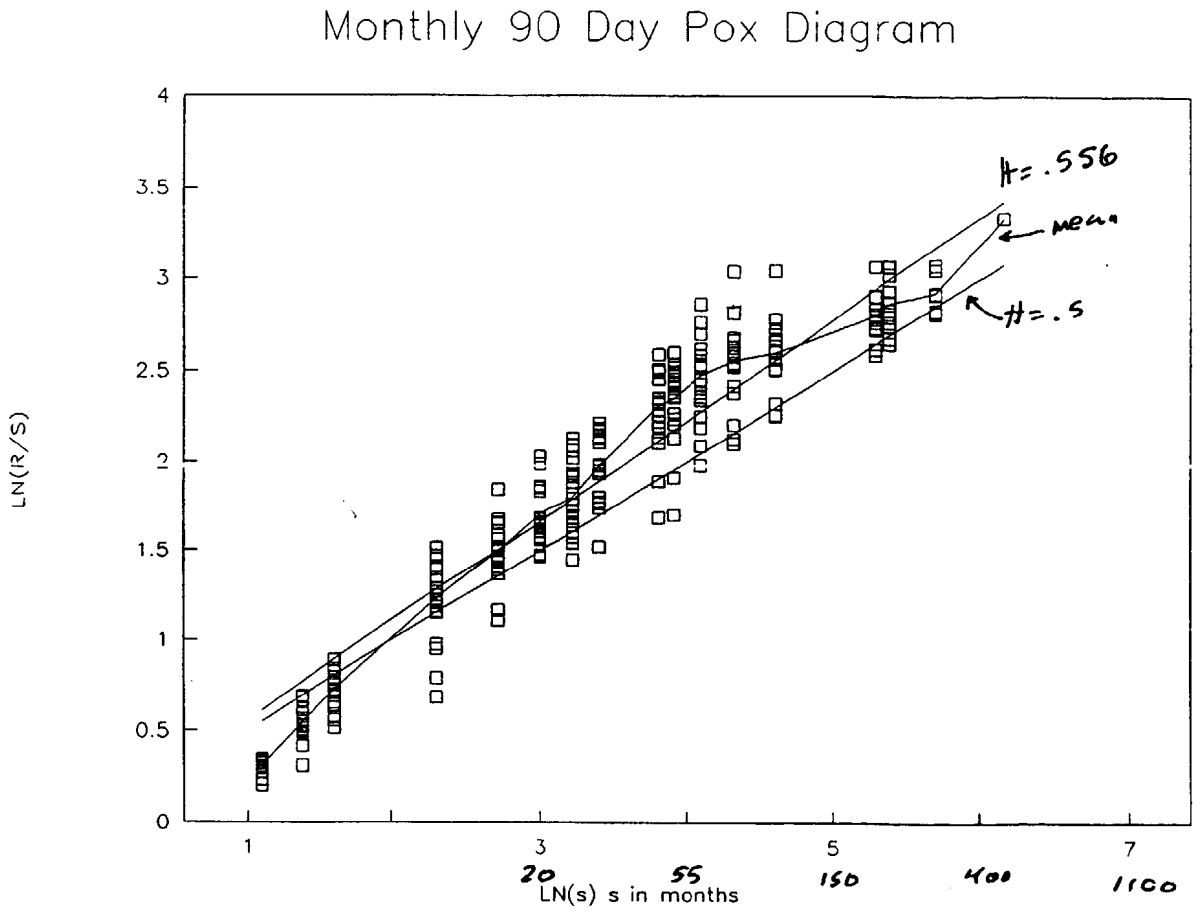
Monthly 90 Day Pox Diagram
LN(R/S)
4
3.5
3
2.5
2
1.5
1
0.5
0
H=.556
mean
H=.5
1
3
5
7
20
55
150
400
1100
LN(s) s in months

Figure 8

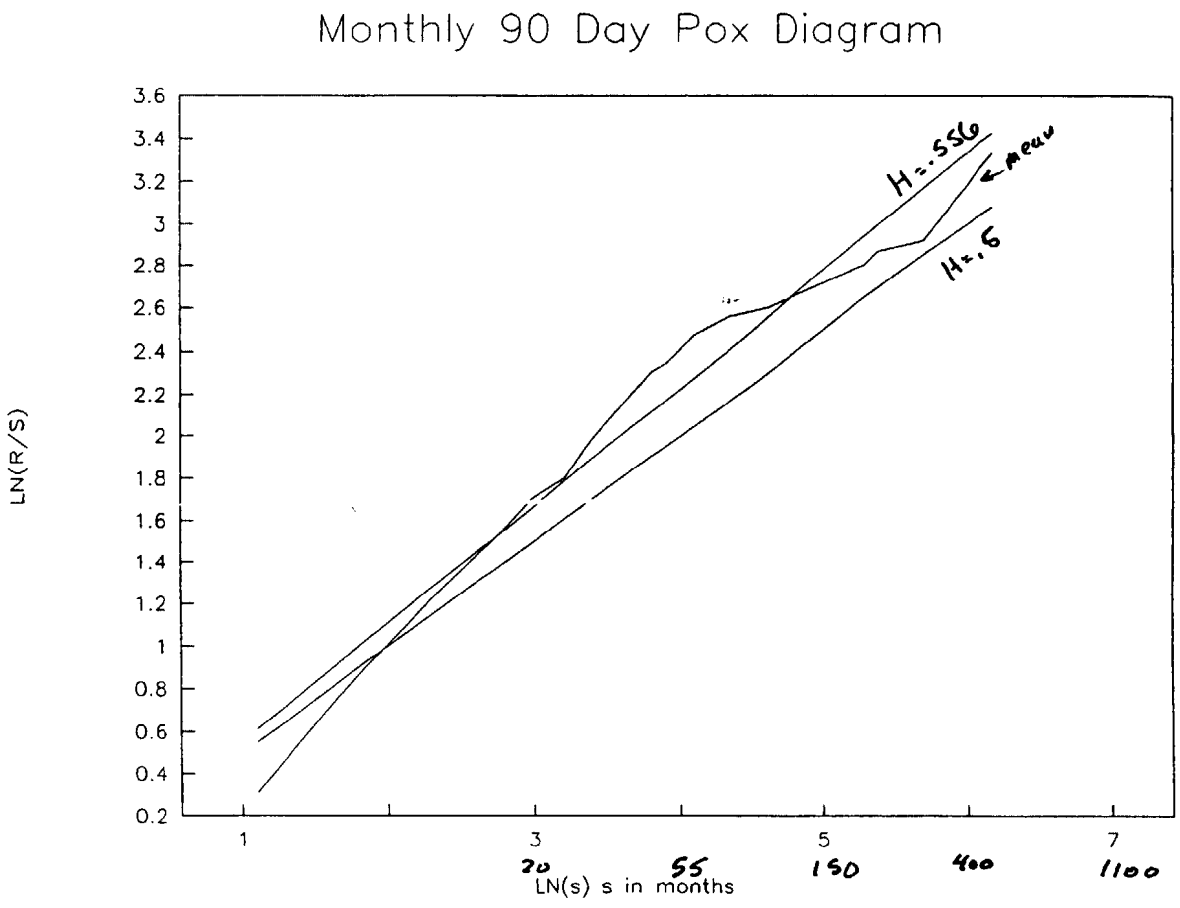
Monthly 90 Day Pox Diagram
LN(R/S)
3.6
3.4
3.2
3
2.8
2.6
2.4
2.2
2
1.8
1.6
1.4
1.2
1
0.8
0.6
0.4
0.2
1
3
5
7
20
55
150
400
1100
LN(s) s in months
H=.556
mean
H=.6

Figure 9

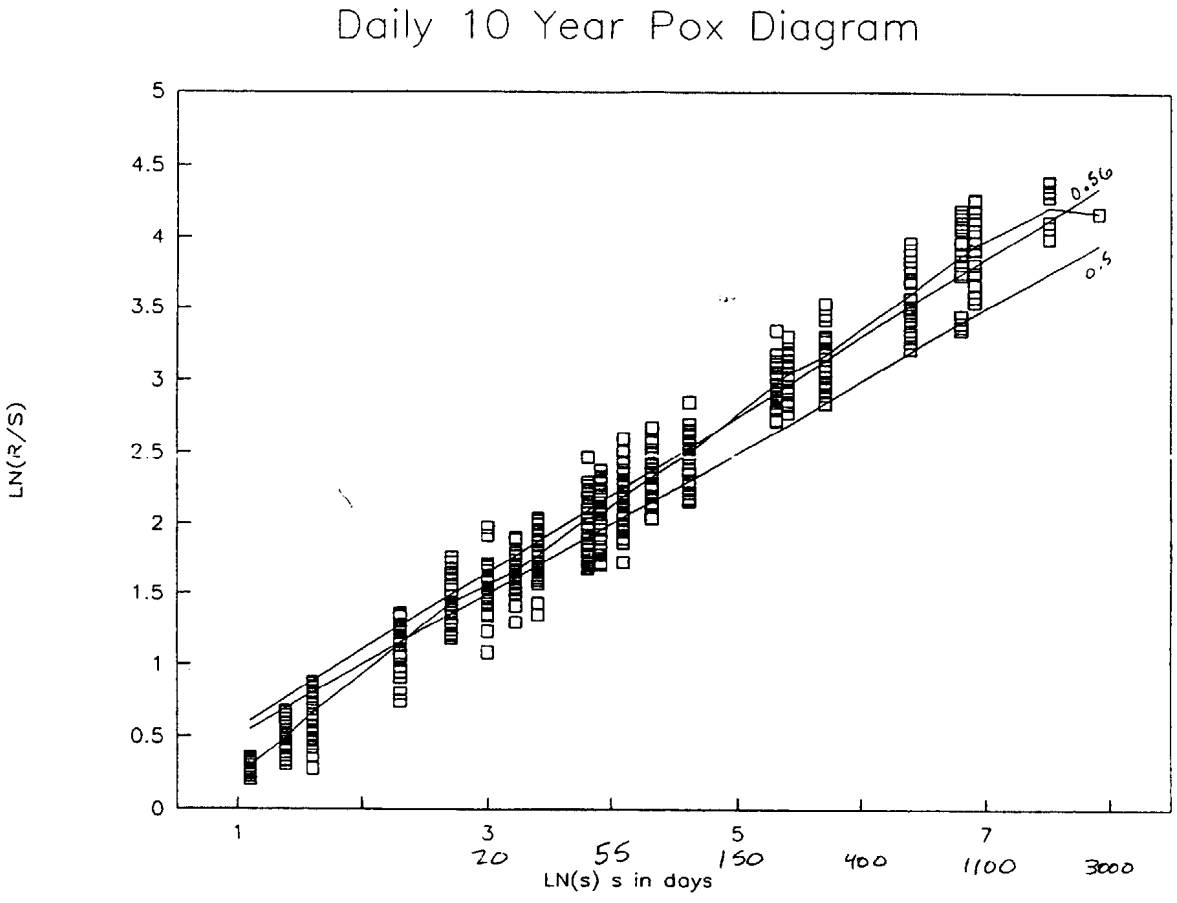
Daily 10 Year Pox Diagram
LN(R/S)
5
4.5
4
3.5
3
2.5
2
1.5
1
0.5
0
0.56
0.5
1
3
20
55
5
150
400
7
1100
3000
LN(s) s in days

Figure 10

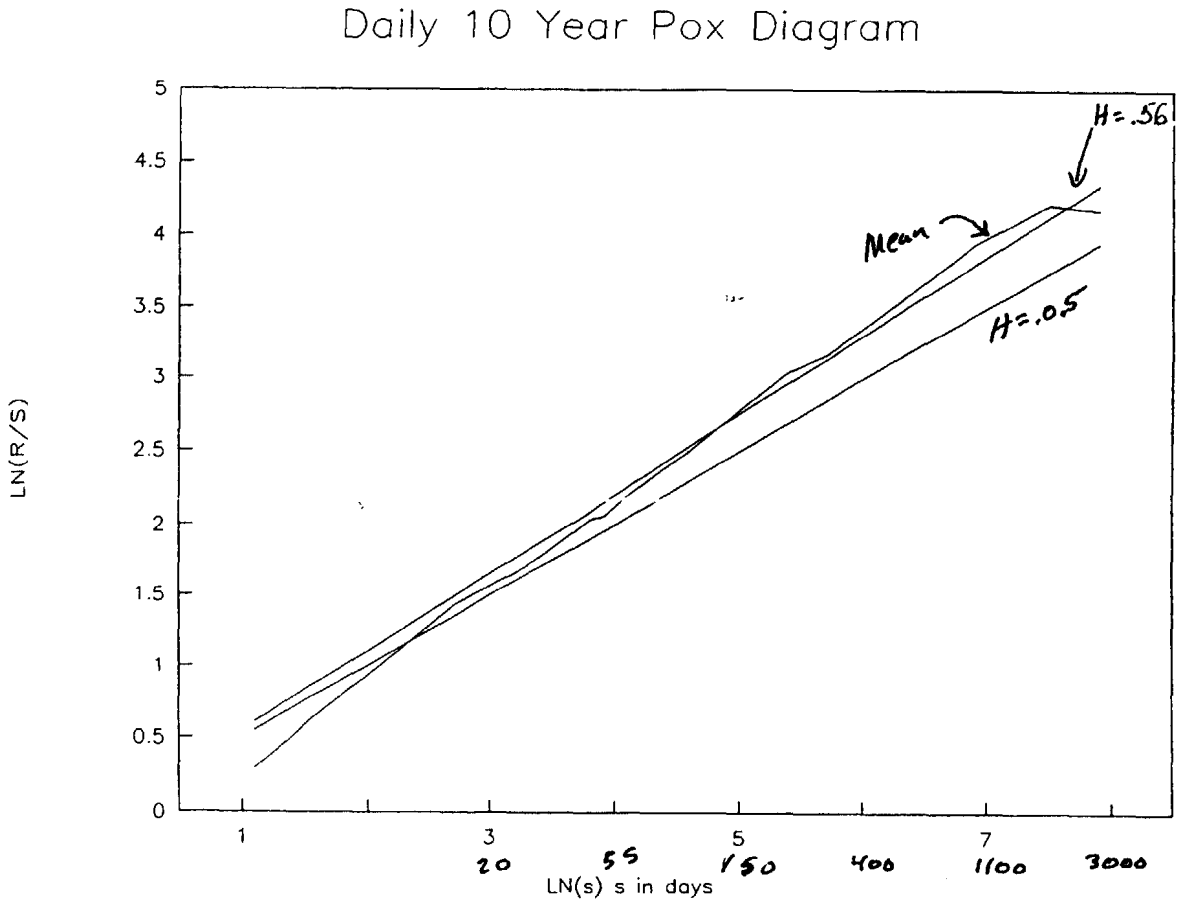
Daily 10 Year Pox Diagram
LN(R/S)
LN(s) s in days
H=.56
Mean
H=.05
0
0.5
1
1.5
2
2.5
3
3.5
4
4.5
5
1
3
5
7
20
55
150
400
1100
3000

Figure 11

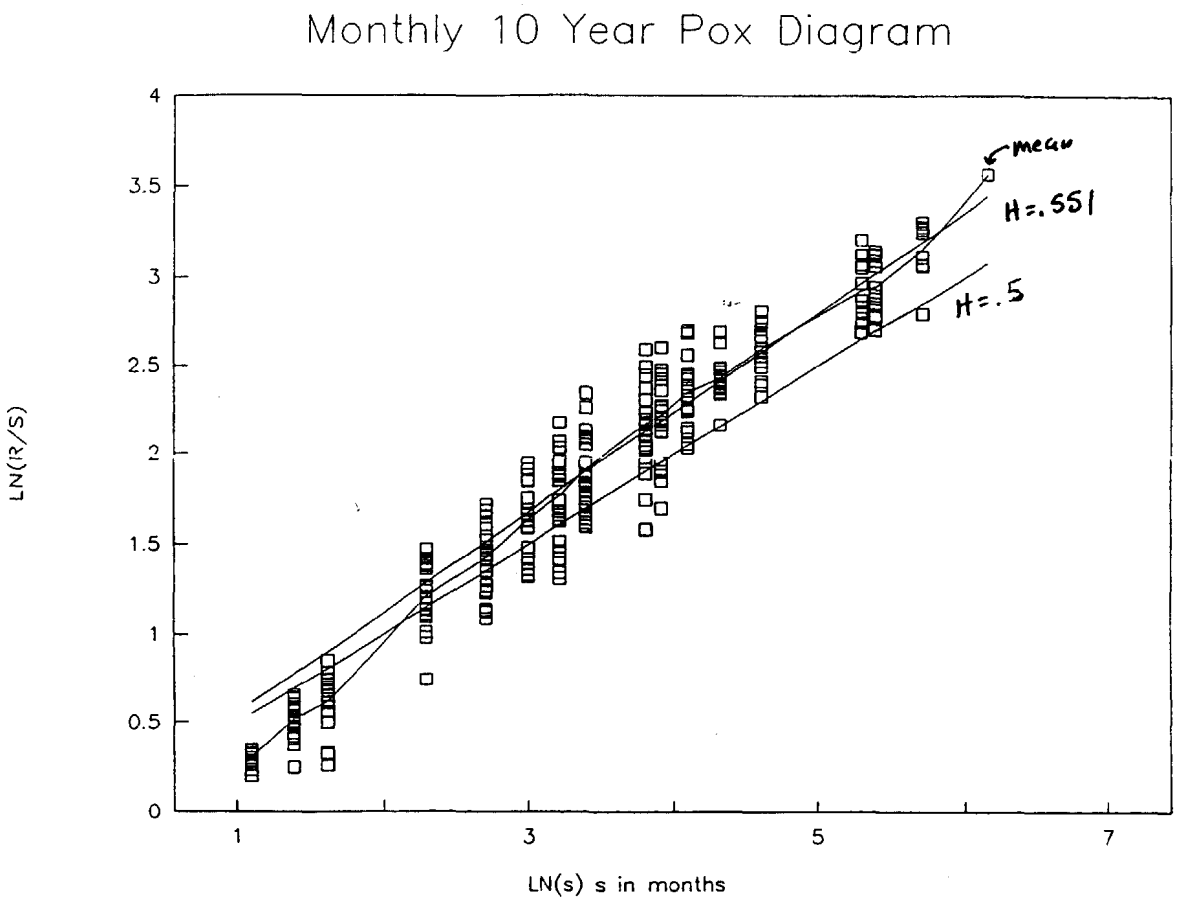
Monthly 10 Year Pox Diagram
LN(R/S)
LN(s) s in months
mean
H=.551
H=.5
0
0.5
1
1.5
2
2.5
3
3.5
4
1
3
5
7

Figure 12

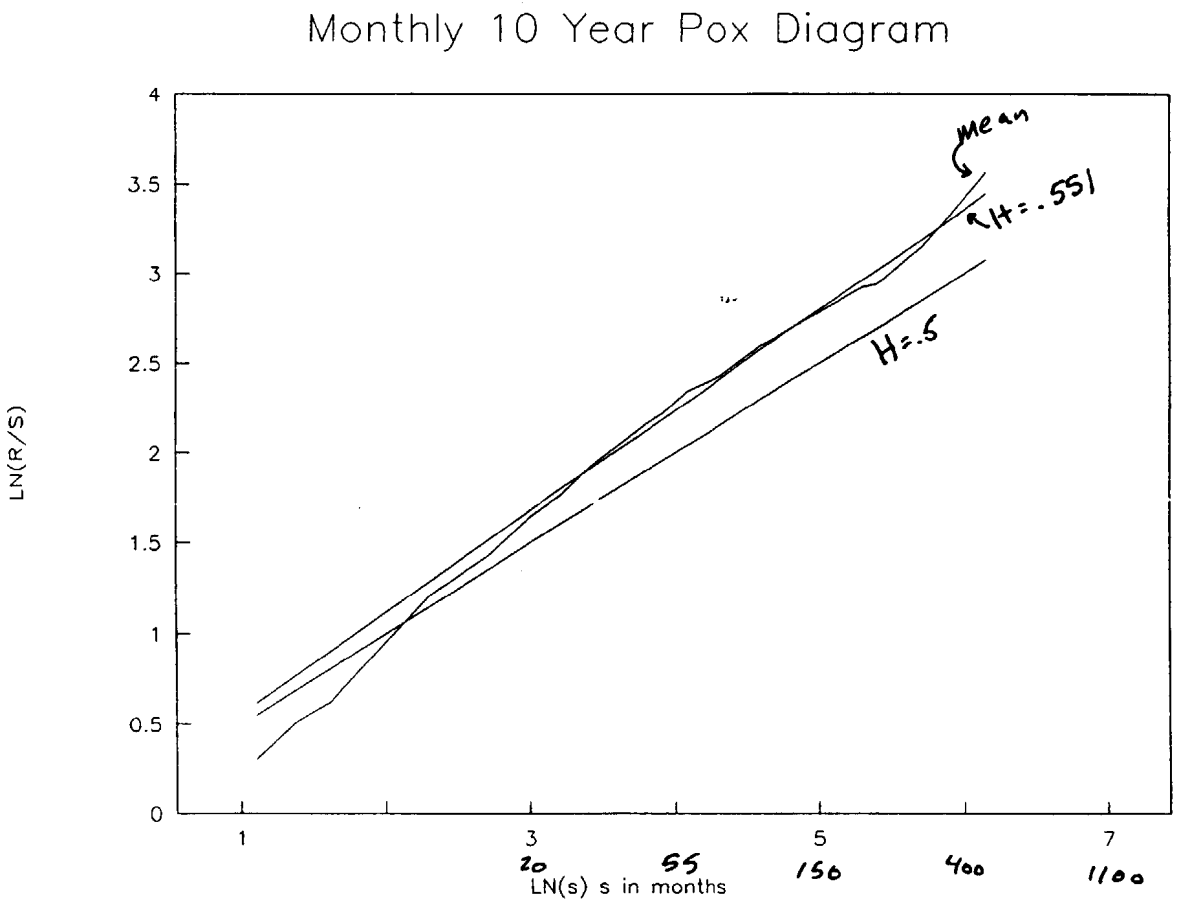
Monthly 10 Year Pox Diagram
LN(R/S)
LN(s) s in months
mean
H=.551
H=.5
4
3.5
3
2.5
2
1.5
1
0.5
0
1
3
5
7
20
55
150
400
1100

Figure 13

regressions. The calculation of the H coefficents excluded all values of $s < 10$. Using a cutoff of 10, instead of 20, caused little information loss from increased variability of the data.

Series	H	Std Err of Coeff	Std Err of Y Est	R^2	Long-term Correlation
$\delta A'$	.553	.004	.08	.994	.075
$\delta B'$	.556	.009	.14	.946	.081
$\delta C'$	.560	.004	.06	.993	.086
$\delta D'$	.551	.004	.10	.991	.073

The H coefficents are significantly away from .5. Since the standard error of the coefficent is a magnitude of 10 less than the difference of H and .5, one can reject the null hypothesis that $H = .5$. Note also the high R^2 value for all the models. However, low correlation indicate that the persistent memory effect is very weak.

Section 6. Conclusions and Further Research

The empirical results suggest several conclusions. First, there is an evident persistent bias that spans decades for both ninety-day and ten-year rates. However, this bias is very weak, implying that the market is nearly efficent. See [31]. In fact one could use H as the measure of market efficiency. The failure of the deterministic chaos algorithms in section 2 also

revalidates some form of the Efficent Market Hypothesis. The closeness of the various H over both the short-term and long-term rates point to the similar marketing of these investment vehicles, or the Federal Reserve's "defensive" purchases and sales of securities. See [39].

Second, the H values are consistent for both the daily and the monthly time series. This result independently verifies the time scale invariance between the different time series.

Third, it is improbable that one can predict interest rates with any accuracy, due to the very low long-term correlation and the fact the the market is nearly efficent. See [36]. Possibly, one could predict the direction of movement. The persistent bias of the FBM creates a weak momentum in the current direction of movement.

Fourth, one can not make any good short term predictions, due to the random nature of the time series for $s < 20$, and the low correlation dimension, from the deterministic analysis. Note the correlation dimension's value is comparable to the long-term correlation for $\delta A'$, note also the auto-correlations are within reason as well.

The results also point to various research possibilities. First, FBM may be a good model for these various time series. The mean zero increment of zero and increasing variance

properties of FBM may explain Becker's observation that the time series, do not follow a lognormal distribution [37]. Note Kapteyn's formula

$$B_H(t) - B_H(t-1) = \Phi\, B_H(t-2) \qquad (6.1)$$

for the law of proportional effect for the lognormal distribution. The formula is similar to formula (3.1) for FBM. See [38]. However, further research on the actual empirical time series is necessary to see if the FBM is either Gaussian or Non-Gaussian. Our formula (3.2), assumes that Φ is from a standard Normal distribution. However, the empirical data for the 90 day rates, shows that the volatility of the rates is greater when the rates are high, and lower when the rates are low. Such behavior does not correspond to a Gaussian FBM. Also, the rates are restrained between 0 and some positive rate (possibly about 25%). However, the FBM as modelled in (3.2) does not have these restraints. This might be overcome by modeling the rates as Log FBM, that is model Exp(Z), where Z is a Gaussian FBM process. This will need to be a topic of a future paper.

Second, many modern financial models, e.g. Black Sholes Option Pricing and its many spinoffs, set up stochastic differential equations. These stochastic differential equations have certain term(s) which follow a pure Brownian Motion model. So, there is potential in modeling these same terms using FBM. This approach may create additional means to eliminate certain market inefficiencies.

Third, one can use this analysis to generate various business scenarios. Simply determine the H exponent, and use formula (3.2), or one similar to it.

Fourth, studies of the H exponent originated with hydrological analysis. Casualty actuaries could use the extensive research in this area, and apply corresponding H exponents for a specific river systems, generating random scenarios to improve flood insurance pricing.

Fifth, in Macroeconomics, the concept of rational expections in the study of inflation states that the expections of inflation are based on all available information, and any expectations of inflation and its actual rate will differ only when a random shock affects the rate. This is also modelled with Brownian Motion, and FBM should be considered. See [40]. Also, FBM should be considered in the modeling of the wage-price spiral. See [41].

Sixth, on a more theorical note, there is a need to generalize R/S analysis into multiple dimensions. Such a theory would aid the analysis of coupled long-term and short-term interest rates.

Acknowledgements: I would like to thank Mike Benson and Steve Sedlak for their insight and advice. I would also like to thank Steve Murphy, Dr. Bob Brown, Bill Chang, Aaron Bush, John Smith and Warren Eng for several discussions while conducting

this research. I would like to thank Russ Osborn for his skillful rewording and revision of the paper, as well as his insight on Efficient Markets. I would like to thank both Sophia Mclellan and Dawn Makad for helping to type in thousands of interest rates. I would also like to thank my wife Patricia for her patience while I went off on different mad escapades, and putting up with my frustration and depression when things went poorly. I also want to thank my close friend Yeshua Ha Maschiach for his continual support and encouragement throughout the entire research project.

Bibliography.

[1] Feder, J. Fractals. Plenum Press, New York. pp. 149-211, pp. 229-243.

[2] Mandlebrot, B. (1983). The Fractial Geometry Of Nature. W. H. Freeman and Company, New York. pp. 247-255, pp. 386-387.

[3] Schroeder, M. Fractals, Chaos, Power Laws: Minutes from an Infinite Paradise. W. H. Freeman and Company, New York. pp. 121-160, p. 220.

[4] Fabozzi, F., Fabozzi, T., and Pollack, I. (editors) (1991), The Handbook of Fixed Income Securities Third Edition. Business One Irwin, Homewood Illinois. p. 181.

[5] U. S. Board of Governors of the Federal Reserve System, "Federal Reserve Statistical Release G. 13," May., 1981 through May, 1992.

[6] U. S. Board of Governors of the Federal Reserve System, "Selected Interest Rates," 1986.

[7] Society of Actuaries, Electronic worksheets. Rates from April 30 1953 to December 1969.

[8] McCaffrey, D., Ellner, S., Gallant, R., and Nychka, D. (1992) Estimating the Lyapunov Exponent of a Chaotic System with Nonparametric Regression. Journal of the American Statistical Assocation. September 1992, Vol. 87, No. 419. pp. 682-695.

[9] Eckmann, J., and Ruelle, D. Ergodic Theory of Chaos and Strange Attractors. Reviews of Modern Physics. July 1985, Vol. 57, No. 3. pp. 617-656.

[10] Eckmann, J., Kamphorst, S., Ruelle, D., and Ciliberto, S. Liapunov Exponents from Time Series. Physical Review A. December, 1986, Vol. 34, No. 6. pp. 4971-4979.

[11] Brown, R., Bryant, P., and Abarbanel, H. Computing the Lyapunov Spectrum of a Dynamical System form an Observed Time Series. Physical Review A. March 1991, Vol. 43, No. 6. pp. 2787-2806.

[12] Farmer, J., and Sidorowich, J. Predicting Chaotic Time Series. Physical Review Letters. August 1987, Vol. 59, No. 8. pp. 845-848.

[13] Sugihara, G., and May, R. Nonlinear Forecasting as a Way of Distinguishing Chaos from Measurement Error in Time Series. Nature. April 1990, Vol 344. pp. 734-741.

[14] Wolf, A., Swift, J., Swinney, H., and Vastano, J. Determining Lyapunov Exponents from a Time Series. Physica D. 1985. pp. 285-317.

[15] Briggs, K. An Improved Method for Estimating Liapunov Exponents of Chaotic Time Series. Physics Letters A. November 1990, Vol. 151, Nos. 1,2. pp. 27-32.

[16] Abarbanel, H., Brown, R., and Kadtke, J. Prediction and System Identification in Chaotic Nonlinear Systems: Time Series with Broadband Spectra. Physics Letters A. July 1989, Vol. 138, No. 8. pp. 401-408.

[17] Casdagli, M. Nonlinear Prediction of Chaotic Time Series. Physica D. 1989, Vol. 35. pp. 335-356.

[18] Packard, N., Crutchfield, J., Farmer, J., and Shaw, R. Geometry from a Time Series. Physical Review Letters. September 1980, Vol. 45, No. 9. pp. 712-716.

[19] Roux, J., Simoyi, R., and Swinney, H. Observation of a Strange Attractor. Physica D. 1983, Vol. 8. pp. 257-266.

[20] Shaw, R. Strange Attractors, Chaotic Behavior, and Information Flow. Z. Naturforsch. 1981, Vol. 36a. pp. 80-112.

[21] Schroeder, M. (Fractals, Chaos, Power Laws op. cit.), p. 220.

[22] Mandlebrot, B., and Wallis, J. (1969) Computer Experiments with Fractional Gaussian Noises. Part 2, Rescaled Ranges and Spectra. Water Resources Research. Vol 5, No. 1 February. pp. 242-259.

[23] Mandlebrot, B. and Van Ness, J. (1968) Fractional Brownian Motions, Fractional Noises and Applications. Siam Review. Vol. 10, No. 4 October. pp. 422-437.

[24] Mandlebrot, B., and Wallis, J. (1969) Computer Experiments with Fractional Gaussian Noises. Part 1, Averages and Variances. Water Resources Research. Vol 5, No. 1 February. pp. 228-241.

[25] Mandlebrot, B., and Wallis, J. (1969) Computer Experiments with Fractional Gaussian Noises. Part 3, Mathematical Appendix. Water Resources Research. Vol 5, No. 1 February. pp. 260-267.

[26] Mandlebrot, B., and Wallis, J. (1969) Some Long-Run Properties of Geophysical Records. Water Resources Research. Vol 5, No. 2 April. pp. 321-340.

[27] Mandlebrot, B., and Wallis, J. (1969) Robustness of Rescaled Range R/S in the Measurement of Noncyclic Long Run Statistical Dependence. Water Resources Research. Vol 5, No. 5 October. pp. 967-988

[28] Feder, J. (Fractals op. cit.), pp. 163-171.

[29] Mandlebrot, B. (1983). (The Fractial Geometry Of Nature op. cit.) pp. 249-250.

[30] Mandlebrot, B. (1983). (The Fractial Geometry Of Nature op. cit.) pp. 248-249.

[31] Peters, E. (1989) Fractal Structure in the Capital Markets. Financial Analysts Journal. July-August pp. 32-37.

[32] Feder, J. (Fractals op. cit.), pp. 173-176.

[33] Mandlebrot, B. (1971) A Fast Fractional Gaussian Noise Generator. Water Resources Research. Vol 7. pp. 543-553.

[34] Feder, J. (Fractals op. cit.), pp. 178-180.

[35] Feder, J. (Fractals op. cit.), pp. 154-162

[36] Bodie, Z., Kane, A., and Marcus, A. (1989) Investments. Irwin, Homewood, Illinois. p. 341-377.

[37] Becker, D. (1991) Statistical Tests of the Lognormal Distribution as a Basis for Interest Rate Changes. Trans. Soc. Actuaries. Vol. XLIII, pp. 7-72.

[38] Crow, E., and Shimizu, K. (editors). (1988) Lognormal Distributions Theory and Applications. Marcel Dekker, Inc., New York. pp. 4-5.

[39] Wachtel, P. Macroeconomics. Society of Actuaries, Schaumburg, Ill. Study note 220-28-91. p. 113

[40] Wachtel, P. (Macroeconomics op. cit.) pp. 86-87.